Published in final edited form as:

Cell Rep. 2023 July 25; 42(7): 112818. doi:10.1016/j.celrep.2023.112818.

A macrophage subpopulation promotes airineme-mediated intercellular communication in a matrix metalloproteinase-9 dependent manner

Raquel Lynn Bowman[1], **Daoqin Wang**[1], **Dae Seok Eom**[1,2,*]

[1]Department of Developmental and Cell Biology, University of California, Irvine, Irvine, CA 92697, USA

[2]Lead contact

SUMMARY

Tissue-resident macrophages are heterogeneous and perform location-dependent functions. Skin resident macrophages play intriguing roles in long-distance intercellular signaling by mediating cellular protrusions called airinemes in zebrafish. These macrophages relay signaling molecules containing airineme vesicles between pigment cells, and their absence disrupts airineme-mediated signaling and pigment pattern formation. It is unknown if the same macrophages control both these signaling and typical immune functions or if a separate subpopulation functions in intercellular communication. With high-resolution imaging and genetic ablation approaches, we identify a macrophage subpopulation responsible for airineme-mediated signaling. These seem to be distinct from conventional skin-resident macrophages by their ameboid morphology and faster or expansive migratory behaviors. They resemble ectoderm-derived macrophages termed metaphocytes. Metaphocyte ablation markedly decreases airineme extension and signaling. In addition, these ameboid/metaphocytes require matrix metalloproteinase-9 for their migration and airineme-mediated signaling. These results reveal a macrophage subpopulation with specialized functions in airineme-mediated signaling, which may play roles in other aspects of intercellular communication.

Graphical Abstract

*Correspondence: dseom@uci.edu.

AUTHOR CONTRIBUTIONS

Conceptualization: R.L.B., D.W., and D.S.E.; investigation: R.L.B., D.W., and D.S.E.; writing – original draft, D.S.E.; writing – review and editing, R.L.B. and D.S.E.; funding acquisition: D.S.E.; supervision: D.S.E.

SUPPLEMENTAL INFORMATION

Supplemental information can be found online at https://doi.org/10.1016/j.celrep.2023.112818.

DECLARATION OF INTERESTS

The authors declare no competing interests.

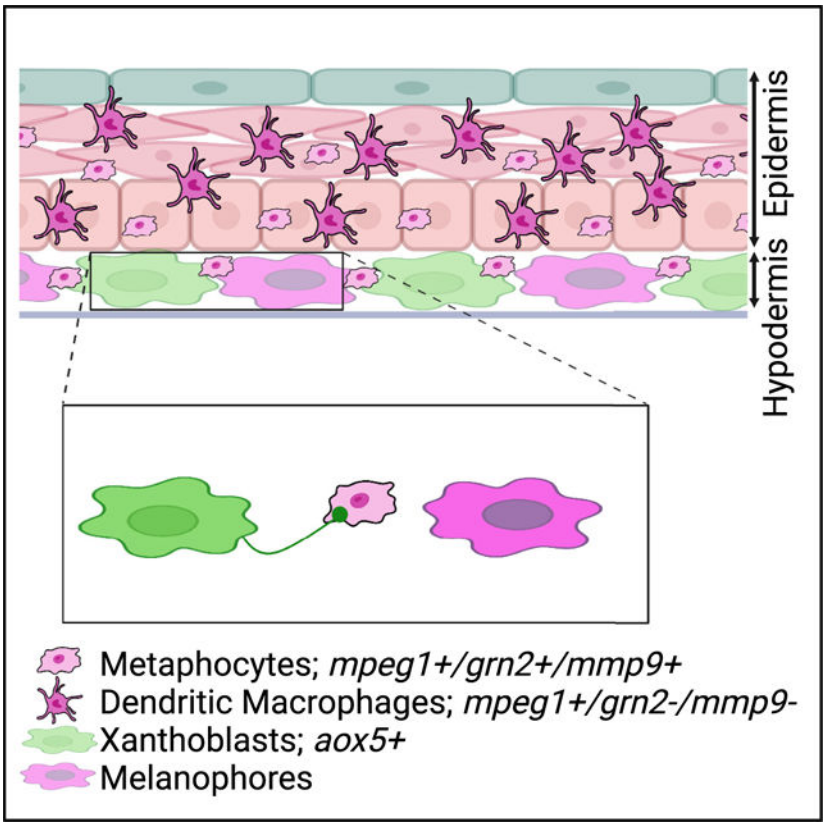

In brief

TRMs are highly heterogeneous and often perform non-immune functions. Bowman et al. discover that metaphocytes, an epithelial-derived macrophage subpopulation, are responsible for airinemes, a long, thin cellular protrusion required for intercellular signaling in zebrafish pigment pattern formation, and their role in airineme-mediated signaling depends on MMP9 activity.

INTRODUCTION

Intercellular signaling in multicellular organisms is essential for development and homeostasis. Uncontrolled regulation of such signaling causes various human diseases, and altered intercellular communication is a hallmark of aging.[1] Intercellular communication mechanisms include endocrine, paracrine, juxtacrine, and neuronal signaling, with diffusion-based local signaling thought to be a dominant dissemination mechanism in paracrine signaling.[2–5] In recent years, growing evidence has suggested that cells can communicate with each other via long, thin cellular protrusions extended by signal sending or receiving cells.[6–9] These can be classified based on their cytoskeletal composition, mode of signal delivery, morphology, and more. The growing list of such protrusions that have been identified include cytonemes, tunneling nanotubes, airinemes, inter-cellular bridges, and migrasomes.[10–13] They are found in a variety of cell types and species, such as fruit fly, sea urchin, zebrafish, and cultured mammalian cells, and their signaling roles have been functionally validated.[14] These signal-carrying protrusions are orders of magnitude

longer than typical filopodia and can extend or retract in a highly dynamic fashion. They directly contact target cells and deliver the major morphogens in many paracrine contexts. In addition, membrane ligand and receptor-mediated intercellular communication, such as Delta-Notch signaling, can also be mediated over long distances via such signaling cellular protrusions.[6,15–17]

Previously, we identified a class of signaling cellular protrusion called airinemes critical for interactions between zebrafish pigment cells. They are unique in having large vesicle-like structures at their tips.[6] They are highly curved, and mathematical models suggest that such complex shapes are optimized to search for target cells.[18] Airinemes preferentially extend from undifferentiated yellow pigment cells, xanthoblasts, and their vesicles contain Delta C ligand, which they deliver to melanophores. Notch activation in target melanophores induces them to migrate from prospective interstripe to stripes, establishing stripe pigment formation. When airineme extensions are inhibited, target melanophores are retained in the interstripe, which leads to failure of proper stripe consolidation. Intriguingly, we have also found that skin-resident macrophages play an essential role in airineme-mediated signaling. Skin-resident macrophages recognize the bulged membrane blebs from the surface of airineme-producing xanthoblasts. These blebs, precursors of airineme vesicles, are grabbed and extracted by macrophages, and, as they migrate, filaments trail behind. Macrophages drag the vesicles along as they migrate through the tissue, deposit them onto the surface of target melanophores, and continue to wander. Thus, the highly curved airineme trajectories observed reflect complex migratory paths of skin-resident macrophages. Deposited vesicles on target melanophores then remain for 1 h or longer, even after filament retraction, an interval presumed to be sufficient for activation of Notch signaling. Afterward, other macrophages phagocytose the deposited airineme vesicles. Thus, macrophages seem to initiate and terminate airineme-mediated long-range Notch-Delta signaling. When the skin-resident macrophages were depleted, airineme extension was markedly decreased, suggesting that macrophages are essential for airineme extension.[6,14,19]

Macrophages are well described immune cells that phagocytose foreign pathogens and apoptotic bodies, critical for self-defense and maintaining homeostasis.[20–23] Tissue-resident macrophages (TRMs) are highly heterogeneous immune populations found in different local niches with unique tissue-specific functions. Unlike conventional macrophages derived from hematopoietic stem cells, TRMs originate in various tissues as shown by fate mapping studies in mice.[24–26] In zebrafish, ectoderm-derived skin resident macrophages are called metaphocytes. Endoderm-derived metaphocytes are also found in the gills and intestine of zebrafish. While metaphocytes express phagocytic genes, they seem not professional phagocytes. Instead, they are specialized for capturing external soluble antigens and transferring them to other immune cells.[27,28]

Prior studies have suggested that, occasionally, the specialized functions of TRMs are not directly involved in immunity.[29] During development, they play essential roles in tissue remodeling.[19,30] Microglia, macrophages in the postnatal brain in mice, for example, are critical for synaptic pruning.[31] Other roles for TRMs include blood vessel pruning and regression and fin regeneration in zebrafish.[32,33] TRMs in skin are essential in airineme-mediated intercellular signaling during postembryonic tissue remodeling.[14,19]

Both typical and atypical functions of macrophages depend on their ability to migrate. Macrophages can infiltrate most tissues and migrate between cells *in vivo* by degrading extracellular matrix with extracellular proteinases such as matrix metalloproteinases (MMPs), cathepsins, and urokinase-type plasminogen activator.[34] A few studies have shown that MMP9 activity is critical in macrophage migration in mice and zebrafish.[35,36]

Here we use high-resolution live imaging and genetic cell ablation to show that a skin-resident macrophage subpopulation resembling metaphocytes is essential in airineme-mediated intercellular communication between pigment cells in zebrafish. Consistent with this hypothesis, metaphocyte-specific ablation abrogates airineme extension and subsequent signaling. Last, we show that the ability of these macrophage subpopulations to mediate airineme signaling depends on MMP9 activity. Our study shows macrophage heterogeneity and the diversity of cellular functions performed by TRMs in cellular protrusion-mediated intercellular signaling.

RESULTS

Two distinct macrophage subpopulations in zebrafish skin

Skin-resident macrophages play essential roles in airineme-mediated long-range intercellular communication.[14,19] Here we asked if the same macrophage population performs both its typical innate immune functions and the airineme-mediated signaling roles or if there are other subpopulations of macrophages specialized for airineme signaling. To look for distinct macrophage subpopulations in the zebrafish skin, we first examined mpeg1+ cells, a widely recognized marker specific to macrophages in zebrafish.[37] We used a transgenic reporter line, Tg(mpeg1:tdTomato), to visualize these cells at the metamorphic stages where macrophage/airineme-mediated signaling most frequently occurs.[6,37] High-resolution, confocal time-lapsed imaging revealed two morphologically distinct mpeg1+ macrophages. The first type includes cells that are relatively large, dendritic, and express a higher level of mpeg1, while the second type is relatively smaller, ameboid in shape, and expresses less mpeg1 (Figures 1A and 1B and Video S1). These two subpopulations also seemed to traverse different depths of the skin, which led us to ask how deep each population traveled, given that airineme-producing xanthoblasts are restricted to the hypodermis. For this, we measured the distance between each macrophage subpopulation and xanthoblasts. While both subpopulations were spread throughout the skin, there were significantly more ameboid cells located basally in the hypodermis than dendritic macrophages found mostly in the epidermis (Figures 1A and 1C). Based on their morphology and relative locations, ameboid and dendritic macrophages seem to be two distinct subpopulations, which led us to ask if these two subpopulations also behave differently. Studying their migration patterns revealed that ameboid macrophages migrate significantly faster than dendritic macrophages (Figure 1D). Strikingly, the migration speed of the ameboid macrophages matched with the speed of airineme extension, indicating that ameboid macrophages were more likely to interact with airineme vesicles than dendritic macrophages at these metamorphic stages.[6]

Ameboid mpeg1+ macrophages interact with airineme vesicles

Indeed, *ex vivo* high-resolution live confocal imaging revealed that ameboid macrophages almost exclusively interacted with airineme vesicles and pull them as compared with dendritic macrophages (Figures 1E and 2F and Video S2, arrowhead). Overall, our observations suggest that, among the two distinct macrophage subpopulations in zebrafish skin, the ameboid macrophage subpopulation preferentially interacts with airinemes.

As mentioned, airinemes extend most frequently during metamorphic stages (SSL 7.5).[6] Thus, we asked if the ameboid subset of macrophages proportionally expands at these stages. However, both overall skin-resident macrophage (mpeg1+) numbers and the ameboid subpopulation increased in similar proportions, with the ameboid population maintained at 24%–29% of total macrophages during SSL5.5–8.5 (Figure S2A).

Airineme-pulling ameboid macrophages overlap with metaphocytes

Traditionally, macrophages have been classified largely into two subpopulations based on their polarization.[20,38,39] Classically activated M1 macrophages are round, while alternatively activated M2 macrophages are more elongated.[23,40] To determine if airineme-associated ameboid macrophages are M1 like, we examined the M1 marker, tumor necrosis factor alpha.[40,41]However, neither ameboid nor dendritic macrophages expressed this marker (Figure S3A). This result is consistent with our previous finding that airineme extension is independent of macrophage activation.[6]

Ectoderm- or endoderm-derived macrophages termed metaphocytes have been recently identified in zebrafish.[27,28,42] Metaphocytes are transcriptionally similar to conventional TRMs in the epidermis[28] and comparable with conventional macrophages, which originate during hematopoiesis.[38] Interestingly, it has been suggested that metaphocytes function by delivering antigens rather than responding to immune-related events. Moreover, their morphology resembles that of the airineme-pulling ameboid macrophage subpopulation (Figures 1A–A′ and Video S2).[27,28,42] Thus, we hypothesized that metaphocytes promote airineme-mediated intercellular signaling. We first tested whether ameboid macrophages express metaphocyte markers. Metaphocyte-specific reporter lines in which EGFP expression is driven by the promoter of either claudin-h (cldnh) or granulin2 (grn2) were crossed with the macrophage reporter, *Tg(mpeg1:tdTomato)*.[27,28] Tg(cldnh:EGFP; mpeg1:tdTomato) and Tg(grn2:EGFP; mpeg1:tdTomato) both label ameboid mpeg1+ macrophages, while dendritic populations do not express either metaphocyte marker (Figure 2A [arrowheads] and Figure S3B). In addition, the number of ameboid macrophages and metaphocytes (grn2+/mpeg1+) at each developmental stage were similar, suggesting that the airineme interacting ameboid macrophage subpopulation largely overlaps with metaphocytes in zebrafish skin (Figure S2B).

We confirmed that metaphocytes associate with airinemes with *ex vivo* live imaging (Figure 2B and Video S3). Furthermore, their distribution among the skin layers is consistent with that of the ameboid population shown in Figure 1C (see also Figure 2C). Thus, if metaphocytes are an airineme-pulling macrophage subpopulation, we expect a significant inhibition of airineme extension in the absence of metaphocytes. To test

this idea, we specifically ablated metaphocytes by using a transgenic line, Tg(grn2:EGFP-v2a-nfsB) that expresses the enzyme nitroreductase (NTR; *nfsB*) in metaphocytes. NTR converts the innocuous prodrug metronidazole into a toxic metabolite that kills cells.[43,44] In conditions where metaphocytes were effectively depleted while xanthoblasts and the dendritic macrophage sub-population remained unaltered (see Methods), we observed a significant reduction in airineme extension (Figures 2D, S4, and Video S5). These findings suggest that the ameboid macrophage subpopulation overlaps with metaphocytes, and they are responsible for airineme-mediated signaling.

Metaphocyte-mediated airineme extension is responsible for pigment pattern development

Airineme-mediated signaling is critical for pigment pattern formation. During metamorphosis, signal molecule-bearing airineme vesicles are relayed to target melanophores by macrophages. The target cells receive signals from airineme vesicles and are directed to migrate out of the interstripe and coalesce into the stripes.[6,14,19] Thus, we asked if metaphocytes are responsible for pigment pattern formation. Repeated metaphocyte ablation during pigment pattern development exhibited melanophore retention in interstripe, while the controls had few to no melanophores at SSL 12 (see Methods).[45] The total numbers of melanophores were not altered in either the controls or the experimental, suggesting airineme target melanophore migration into stripes was hindered in the absence of metaphocytes (Figure 3A and 3B). The disorganized pigment patterns observed resembled the phenotypes found when airinemes were inhibited, or all mpeg1+ macrophages in the skin were depleted.[6,19] Our data suggest that metaphocytes are responsible for pigment pattern formation via airineme-mediated signaling.

Metaphocyte migration and airineme extension are MMP9 dependent

We asked what underlying molecular mechanism differentiates ameboid/metaphocytes from the dendritic macrophage subpopulation. MMPs are a critical component of macrophage migration. Among many MMPs, MMP9 has been suggested to be required for macrophage migration and phagocytosis.[35,36] Therefore, we hypothesized that differential MMP9 requirement governs migratory behavior between ameboid/metaphocytes and dendritic macrophages in zebrafish skin. To test if *mmp9* is differentially expressed in these two macrophage subpopulations, we generated Tg(mmp9:EGFP; mpeg1:tdTomato), which labels both macrophage subpopulations and *mmp9*-positive cells.[46] We observed that ameboid/metaphocytes exhibited strong *mmp9* expression, but the dendritic population showed no detectable reporter expression (Figures 4A, S3B, and S3C). Consistently, only ameboid/metaphocyte migration speed was significantly decreased in the presence of MMP9 inhibitor. However, dendritic cell migration was unchanged, suggesting that MMP9 is indispensable for ameboid/metaphocyte migration (Figures 4B and 4C and S5). Consistent with airinemes interacting specifically with ameboid/metaphocytes, we observed similar decreases in airineme extension speed in the presence of an MMP9 inhibitor (Figure 4D). Surprisingly, we discovered that airineme extension frequency was significantly compromised upon treatment with this MMP9 inhibitor (Figure 4E and Video S6). We reasoned this might be caused by the drug preventing metaphocyte infiltration into the hypodermis. Indeed, we observed that the localization of ameboid/metaphocytes along the apical-basal axis was shifted apically in the presence of MMP9 inhibitor compared with

controls. Thus, limited access of ameboid/metaphocytes to the hypodermal layer could cause the significant decreases in airineme extension frequency seen in MMP9 inhibitor-treated animals (Figure 4F). Last, we observed that the airineme extension was significantly reduced when we ablated *mmp9*+ cells with Tg(mmp9:nfsB-EGFP)[46] (Figures 4G, S5 and Video S5). Furthermore, we observed similar melanophore retention in the interstripe of *mmp9*+ cell-depleted fish, resembling the effect seen in metaphocyte depletion (Figure S6). However, we did not detect any significant changes in the proportion of both macrophage populations or morphological alterations, as assessed by quantifying the number and the length of protrusions in both populations (Figures S7A, S7B, and S7C).

To further confirm the role of *mmp9* in metaphocytes, we over-expressed *mmp9* in both macrophage subpopulations, *Tg(mpeg1:mmp9-v2a-nVenus)*. We observed an increase in airineme extension in the *mmp9* overexpressed fish (Figure 4H). Expectedly, the migration speed of the ameboid population was significantly increased, and the dendritic cells remained unaffected in this transgenic line (Figure 4I). However, both ameboid and dendritic macrophage populations did not show significant changes in their localization within the skin layers and proportion of both macrophage population (Figures S7D and S7E). We speculate that the increased migration speed of metaphocytes enhances their chances of contacting airineme blebs on the surface of xanthoblasts, resulting in a higher incidence of airineme extension.

Together, these findings suggest that ameboid/metaphocyte-mediated airineme signaling depends on MMP9 activity.

DISCUSSION

Several features of airinemes distinguish them from other signaling cellular protrusions, such as cytonemes and tunneling nanotubes. One of the most striking differences is that airinemes require macrophages as delivery vehicles for relaying airineme vesicles to the target melanophores intermingled with non-target cells.[11,14] Airinemes may need these cells to help them extend through the densely packed tissue environment, especially airinemes with large vesicles at their tips.[47]

Our study suggests that ameboid macrophages/metaphocytes in metamorphic zebrafish skin specifically perform such a delivery role in airineme signaling. We have shown that the behaviors of this macrophage subpopulation correlate with airineme-mediated signaling since they migrate faster and can infiltrate deeper into hypodermis than the dendritic subpopulation. Our study also suggests that MMP9-dependent migration of metaphocytes is critical for airineme-mediated intercellular communication. However, dendritic macrophages do not seem to express MMP9, and their migration was not affected by both MMP9 inhibitor treatment and *mmp9* overexpression. Additionally, it has been observed that *mmp9* does not play a role in the fate determination between metaphocytes and dendritic macrophages (Figures S7A and S7E). There are 26 MMP-orthologs in zebrafish and 24 different MMP genes in humans. Thus, it will be interesting to study whether combinatorial MMP expression control or finetune macrophages' migratory behaviors in different subpopulations

or disease contexts. This idea is supported by studies showing that MMP-mediated macrophage infiltration is associated with various human pathophysiologies.[48–50]

Our results are consistent with previous reports showing that ameboid/metaphocytes are specialized for antigen delivery, but less reactive to immunogenic processes.[28] Metaphocytes in metamorphic zebrafish skin is also specialized for airineme vesicle delivery. However, from our previous studies, we observed that metaphocytes engulf and eliminate the airineme vesicles when they are docked on non-target cells, suggesting they are still phagocytes. However, airineme vesicles are not phagocytosed while airinemes extend and when they contact target cells.[6,19] Thus, it seems that the target recognition mechanism is tightly linked to determining metaphocytes to phagocytose the airineme vesicles. We speculate that these ameboid/metaphocytes control target recognition in airineme-mediated intercellular communication. One possibility is that metaphocytes scan the surfaces of cells along their migration paths and deposit airineme vesicles onto specific target melanophores. Thus, cell membrane receptor/ligand interactions between metaphocytes and target cells might provide a cue for target cell specificity, and this might prevent airineme vesicle phagocytosis. Alternatively, it is possible that interactions between airineme vesicles and target cell membranes underlie this target specificity and metaphocytes simply act as delivery vehicles. However, the molecular mechanisms behind metaphocytes' target-specific behaviors remain to be elucidated.

We identified two distinct macrophage subpopulations in metamorphic zebrafish skin, consistent with previous descriptions of metaphocytes in adult zebrafish.[27,28] However, the localization of metaphocytes in adults is near the peridermal epidermis and conventional dendritic macrophages stay relatively more basally, while we find that our ameboid, metaphocyte-like cells lie more basally than dendritic macrophages (Figures 1C and 2C). This discrepancy may simply reflect stage-dependent differences in these cell types. In our study, we have shown that airinemes are most frequently observed during metamorphosis, where robust tissue remodeling, including pigment pattern formation, occurs, but their extension frequency diminishes as fish develop.[6] Thus, it is conceivable that metaphocytes repurpose their function to relay antigens in adult zebrafish skin.

It is important to note that, in rare cases, we observed ameboid macrophages that did not express metaphocyte markers. We also observed that *grn2*+ metaphocytes displayed a varying degree of reporter expression in the transgenic lines. This may reflect their maturation status or suggest the existence of additional macrophage subpopulations. However, these nonmetaphocyte ameboid macrophages make up a much smaller portion than most ameboid/*grn2*+ metaphocytes in metamorphic zebrafish skin.

Taken together, our study revealed that airineme-vesicles interact specifically with an ameboid macrophage subpopulation, most likely ectoderm-derived macrophages called meta-phocytes. Moreover, metaphocytes are responsible for airineme-mediated signaling via MMP9 activity-dependent fashion. Our study suggests that macrophage involvement in airineme-mediated signaling is not an experimental side effect but highly regulatory and that airinemes achieve intercellular signaling by using TRM heterogeneity and versatility. Our study also demonstrates the complex and cooperative nature of the cellular protrusion-

based intercellular signaling between pigment cells in zebrafish skin. Requirements for macrophages in other cellular protrusion-mediated signaling modalities are unknown, which is an interesting avenue for future studies.

Limitations of the study

Although we have provided multiple lines of evidence suggesting that the dendritic macrophage subpopulation does not seem to contribute to airineme extension and signaling, we were unable to directly test this hypothesis through dendritic macrophage-specific ablation experiments. This limitation primarily arose from the lack of reliable and specific transgenic lines available for metamorphic zebrafish.

STAR★METHODS

RESOURCE AVAILABILITY

Lead contact—Further information and requests for resources and reagents should be directed to and will be fulfilled by the lead contact, Dae Seok Eom (dseom@uci.edu).

Materials availability—This study generated two zebrafish transgenic lines, *Tg(mpeg1:mmp9-v2a-nVenus)irrt15Tg* and *Tg(krt4:palmEGFP)irrt1Tg*, and a construct *cldnh:mCherry*. They are available from the lead contact without restriction.

Data and code availability

- All original data reported in this paper will be shared by the lead contact upon request.
- No original code has been generated in this study.
- Any additional information required to reanalyze the data reported in this paper is available from the lead contact upon request.

EXPERIMENTAL MODEL AND SUBJECT DETAILS

Zebrafish—Fish were maintained at 28.5 C, 16:8 L:D. Zebrafish were wild-type AB^{wp} or its derivative WT (ABb), as well as, *Tg(cldnh:EGFP)*, *Tg(grn2:EGFP;mpeg1.1:LoxP-DSRedx-LoxP-EGFP), Tg(grn2:EGFP-v2a-nfsB)*^{hkz34}, provided by Z. Wen,[27,28] *Tg(tyrp1b:palmmcherry)*$^{wp.rt11,6}$ *Tg(mpeg1:Brainbow)*^{w201}, which expresses tdTomato in the absence of Cre-mediated recombination[51]; *Tg(mmp9:EGFP)*^{tyt206}, *Tg(mmp9:EGFP-v2a-nfsB)*^{tyt207}, provided by A. Kawakami.[46] *Tg(krtt1c19e:lyn-tdtomato)*^{sq16} was provided by T. Carney.[52] Experiments were performed prior to the development of secondary sexual characteristics, so the number of females and males used in the study could not be determined, however, all stocks used generated approximately balanced sex ratios, so the experiments likely sampled similar numbers of females and males. All animal work in this study was conducted with the approval of the University of California Irvine Institutional Animal Care and Use Committee (Protocol #AUP-22–023) in accordance with institutional and federal guidelines for the ethical use of animals.

METHOD DETAILS

Transgenesis and transgenic line production

Tg(krt4:PALMegfp): We acquired Gateway 5′ entry vector p5E:krt4 construct from T. Carney.[52] This construct was assembled with it middle entry vector, pME:PALMegfp and p3E:polyA into pDest backbone. *Tg(mpeg1:mmp9-v2a-nVenus)*: To examine the impact of *mmp9* overexpression in both dendritic and ameboid macrophage subpopulations, we generated *mpeg1:mmp9-v2a-nVenus* construct using Gateway assembly into Tol2 backbone and injected into WT(ABb). The *mmp9* cDNA (ZDB-GENE-040426–2132) was isolated out of cDNA from WT(ABb). The resulting constructs included a Tol2 sequence which allowed for utilization of the Tol2 transposon system to randomly incorporate the plasmid of interest into WT(ABb) fish.

cldnh:mcherry construct: The same *cldnh:EGFP* construct was subcloned to generate *cldnh:mCherry* to label *cldnh* positive cells other than green fluorescent protein using Gibson assembly.[53]

Drug treatments

Metaphocyte long-term ablation: Fish were treated with drugs during dark cycles and then washed and changed into system water without drugs at light cycles. *Tg(grn2:EGFP-v2a-nfsB)* fish were split into two groups: DMSO control and metronidazole (Mtz)-treated experimental, and WT(ABb) were used as an additional control group to assess off target effects of Mtz. Fish in Mtz groups were given 7mM of Mtz dissolved in DMSO. Fish from each group began treatment starting from SSL 7.0 and continued to receive treatment until reaching SSL 12.0. During treatment fish were fed 3 times per day using 1–2 drops of brine shrimp. Upon reaching SSL 12.0, fish were euthanized using tricaine and embedded into a 1% agarose gel in a sterile Petri dish. Colored images were taken using a Koolertron LCD digital microscope.

Overnight treatments: Metaphocytes were ablated overnight for time lapse imaging using fish injected with *aox5:palmEGFP* into *Tg(grn2:EGFP-v2a-nfsB)*. Fish were treated with either 10 mM Mtz or DMSO as a control. MMP9+ cells were ablated for time lapse imaging using fish injected with *aox5:palmEGFP* into *Tg(mmp9:EGFP-v2a-nfsB)*. Fish were treated with either 5 mM Mtz or DMSO as a control. MMP9 inhibition for overnight time lapse was using fish injected with *aox5:palmEGFP* into *Tg(mpeg1:tdtomato)* or WT. Fish were treated with either 0.1 mM MMP9 inhibitor II or DMSO as a control.

Time-lapse and still imaging: *Ex vivo* imaging of pigment cells and macrophages was done using a Leica TCS SP8 confocal microscope equipped with a resonant scanner and two HyD detectors. Time-lapse images taken at 5-min intervals over a span of 10 h. Overnight time-lapse imaging was performed when larvae reached SSL 7.5 except where indicated.[6,19] NTR ablation experiments were performed by administering either 10 mM Mtz into *Tg(grn2:EGFP-v2a-nfsB)* or 5 mM, *Tg(mmp9:EGFP-v2a-nfsB)* overnight for airineme extension frequency measures.

Cell counts and distributions

Pigment pattern: Fish were imaged upon reaching SSL 12.0. Images were taken of the entire trunk and were later cropped to include only the area underneath the dorsal fin. Total melanophore counts and melanophores in the interstripe region were quantified using the cell counter plugin from ImageJ. Total number of melanophores and melanophores in the interstripe region were averaged.

Developmental stage cell population counts: Dendritic and ameboid cell populations were quantified using the cell counter plugin from ImageJ. Dendritic cells were determined by several characteristics including *mpeg1+* (ameboid & dendritic macrophages) reporter expression level, cell morphology, migration speed, branching. Total numbers for each group were averaged across individuals. *gnr2+* cells (metaphocytes) were also quantified using the cell counter plugin of ImageJ and averaged across individuals.

Axial localization of skin-resident macrophages: Localization of ameboid and dendritic populations was determined using z stack information provided by images taken on Leica TCS SP8 confocal microscope. Distance from the hypodermis was measured and determined by co-injected *aox5:palmEGFP+* cells. Thus, smaller numbers indicate closer to the hypodermis and larger numbers closer to the epidermis.

Reverse transcription polymerase chain reaction (RT-PCR) analysis of gene expression in zebrafish skin—Fish at SSL 7.5 were skinned (n = 10) and treated with 500uL of 0.05% Trypsin in phosphate buffer saline (PBS) for 3 min at 28°C to dissociate the cells. Cell dissociation was subsequently stopped by adding 500uL of 1X Defined Trypsin Inhibitor (DTI). Tissues were further lysed at room temperature through the addition of 1 mL TRIzol reagent. After, the sample was treated using 0.2 mL chloroform and the top layer was extracted to obtain total RNA. Samples were cleaned using cold isopropanol and ethanol washes. cDNA was synthesized using a SuperScript III cDNA synthesis kit (ThermoFisher). Amplifications were 35 cycles *(actin, mmp9, aox5, pmela)* at 98°C, 30s; 98°C, 10s; 72°C, 10s; 72°C, 20s; 72°C, 2m; 4°C, hold. *aox5 (*5′-CAGAGTGACGTCTGGTCTTACG-3′; 5′-GGACATCTGATAGCCACACTTG-3′), *pmela* (5′-CTCGGAGTTCTGTTTTTCGTTT-3′, 5′-AAGGTACTGCGCTTATTCCTGA-3′), *actin* (5′-CTTGCTC CTTCCACCATGAA-3’; 5′-CTGCTTGCTGATCCACATCT-3′), *mmp9* (5′-CATTAAAGATGCCCTGATGTATCCC-3’; 5′-AGTGGTGGTCCGTGGTTGAG-3′).

QUANTIFICATION AND STATISTICAL ANALYSIS

Statistical analyses were performed using GraphPad Prism software version 9.0 for Mac (GraphPad Software, San Diego, CA, USA). Continuous data were displayed as mean ± SEM, using an unpaired two-tailed Student’s t-test.

Supplementary Material

Refer to Web version on PubMed Central for supplementary material.

ACKNOWLEDGMENTS

We thank Dr. T. Schilling for critical reading and Dr. J. Lee for valuable discussion. We acknowledge support from NIH MIRA R35GM142791 to D.S.E. We thank the Dr. Wen in Hong Kong University of Science and Technology for sending us *Tg(grn2:EGFP)*, *Tg(grn2:EGFP-nfsB)*, *cldnh:EGFP*, and National BioResource Project, Zebrafish, Core Institution (NZC) in Japan for providing us *Tg(mmp9:EGFP)* and *TG(mmp9:EGFP-nfsB)* lines. We thank Dr. Roh-Johnson at the University of Utah for sending us *TNFα:emGFP* construct.

INCLUSION AND DIVERSITY

We support inclusive, diverse, and equitable conduct of research.

REFERENCES

1. López-Otín C, Blasco MA, Partridge L, Serrano M, and Kroemer G (2013). The hallmarks of aging. Cell 153, 1194–1217. 10.1016/j.cell.2013.05.039. [PubMed: 23746838]
2. Lander AD, Nie Q, and Wan FYM (2002). Do morphogen gradients arise by diffusion? Dev. Cell 2, 785–796. 10.1016/s1534-5807(02)00179-x. [PubMed: 12062090]
3. Müller P, and Schier AF (2011). Extracellular movement of signaling molecules. Dev. Cell 21, 145–158. 10.1016/j.devcel.2011.06.001. [PubMed: 21763615]
4. Wolpert L (1973). Role of diffusible gradients in regeneration. Dev. Biol 30. concl4–5.
5. Wolpert L (2009). Diffusible gradients are out - an interview with Lewis Wolpert. Interviewed by Richardson, Michael K. Int. J. Dev. Biol 53, 659–662. 10.1387/ijdb.072559mr. [PubMed: 19557674]
6. Eom DS, Bain EJ, Patterson LB, Grout ME, and Parichy DM (2015). Long-distance communication by specialized cellular projections during pigment pattern development and evolution. Elife 4, e12401. 10.7554/eLife.12401. [PubMed: 26701906]
7. Ljubojevic N, Henderson JM, and Zurzolo C (2021). The Ways of Actin: Why Tunneling Nanotubes Are Unique Cell Protrusions. Trends Cell Biol. 31, 130–142. 10.1016/j.tcb.2020.11.008. [PubMed: 33309107]
8. Roy S, Huang H, Liu S, and Kornberg TB (2014). Cytoneme-mediated contact-dependent transport of the Drosophila decapentaplegic signaling protein. Science 343, 1244624. 10.1126/science.1244624.
9. Stanganello E, and Scholpp S (2016). Role of cytonemes in Wnt transport. J. Cell Sci 129, 665–672. 10.1242/jcs.182469. [PubMed: 26823607]
10. Caviglia S, and Ober EA (2018). Non-conventional protrusions: the diversity of cell interactions at short and long distance. Curr. Opin. Cell Biol 54, 106–113. 10.1016/j.ceb.2018.05.013. [PubMed: 29890397]
11. Daly CA, Hall ET, and Ogden SK (2022). Regulatory mechanisms of cytoneme-based morphogen transport. Cell. Mol. Life Sci 79, 119. 10.1007/s00018-022-04148-x. [PubMed: 35119540]
12. González-Méndez L, Gradilla AC, and Guerrero I (2019). The cytoneme connection: direct long-distance signal transfer during development. Development 146, dev174607. 10.1242/dev.174607. [PubMed: 31068374]
13. Jiang D, Jiang Z, Lu D, Wang X, Liang H, Zhang J, Meng Y, Li Y, Wu D, Huang Y, et al. (2019). Migrasomes provide regional cues for organ morphogenesis during zebrafish gastrulation. Nat. Cell Biol 21, 966–977. 10.1038/s41556-019-0358-6. [PubMed: 31371827]
14. Eom DS (2020). Airinemes: thin cellular protrusions mediate long-distance signalling guided by macrophages. Open Biol. 10, 200039. 10.1098/rsob.200039.
15. Cohen M, Georgiou M, Stevenson NL, Miodownik M, and Baum B (2010). Dynamic filopodia transmit intermittent Delta-Notch signaling to drive pattern refinement during lateral inhibition. Dev. Cell 19, 78–89. 10.1016/j.devcel.2010.06.006. [PubMed: 20643352]
16. De Joussineau C, Soulé J, Martin M, Anguille C, Montcourrier P, and Alexandre D (2003). Delta-promoted filopodia mediate long-range lateral inhibition in Drosophila. Nature 426, 555–559. 10.1038/nature02157. [PubMed: 14654840]

17. Huang H, and Kornberg TB (2015). Myoblast cytonemes mediate Wg signaling from the wing imaginal disc and Delta-Notch signaling to the air sac primordium. Elife 4, e06114. 10.7554/eLife.06114. [PubMed: 25951303]

18. Park S, Kim H, Wang Y, Eom DS, and Allard J (2022). Zebrafish airinemes optimize their shape between ballistic and diffusive search. Elife 11, e75690. 10.7554/eLife.75690. [PubMed: 35467525]

19. Eom DS, and Parichy DM (2017). A macrophage relay for long-distance signaling during postembryonic tissue remodeling. Science 355, 1317–1320. 10.1126/science.aal2745. [PubMed: 28209639]

20. Guilliams M, Thierry GR, Bonnardel J, and Bajenoff M (2020). Establishment and Maintenance of the Macrophage Niche. Immunity 52, 434–451. 10.1016/j.immuni.2020.02.015. [PubMed: 32187515]

21. Herbomel P, and Levraud JP (2005). Imaging early macrophage differentiation, migration, and behaviors in live zebrafish embryos. Methods Mol. Med 105, 199–214. 10.1385/1-59259-826-9:199. [PubMed: 15492397]

22. Herbomel P, Thisse B, and Thisse C (1999). Ontogeny and behaviour of early macrophages in the zebrafish embryo. Development 126, 3735–3745. 10.1242/dev.126.17.3735. [PubMed: 10433904]

23. Varol C, Mildner A, and Jung S (2015). Macrophages: development and tissue specialization. Annu. Rev. Immunol 33, 643–675. 10.1146/annurev-immunol-032414-112220. [PubMed: 25861979]

24. Ginhoux F, and Guilliams M (2016). Tissue-Resident Macrophage Ontogeny and Homeostasis. Immunity 44, 439–449. 10.1016/j.immuni.2016.02.024. [PubMed: 26982352]

25. Perdiguero EG, Klapproth K, Schulz C, Busch K, de Bruijn M, Rodewald HR, and Geissmann F (2015). The Origin of Tissue-Resident Macrophages: When an Erythro-myeloid Progenitor Is an Erythro-myeloid Progenitor. Immunity 43, 1023–1024. 10.1016/j.immuni.2015.11.022. [PubMed: 26682973]

26. Schulz C, Gomez Perdiguero E, Chorro L, Szabo-Rogers H, Cagnard N, Kierdorf K, Prinz M, Wu B, Jacobsen SEW, Pollard JW, et al. (2012). A lineage of myeloid cells independent of Myb and hematopoietic stem cells. Science 336, 86–90. 10.1126/science.1219179. [PubMed: 22442384]

27. Lin X, Zhou Q, Lin G, Zhao C, and Wen Z (2020). Endoderm-Derived Myeloid-like Metaphocytes in Zebrafish Gill Mediate Soluble Antigen-Induced Immunity. Cell Rep. 33, 108227. 10.1016/j.celrep.2020.108227. [PubMed: 33027664]

28. Lin X, Zhou Q, Zhao C, Lin G, Xu J, and Wen Z (2019). An Ectoderm-Derived Myeloid-like Cell Population Functions as Antigen Transporters for Langerhans Cells in Zebrafish Epidermis. Dev. Cell 49, 605–617.e5. 10.1016/j.devcel.2019.03.028. [PubMed: 31006648]

29. Blériot C, Chakarov S, and Ginhoux F (2020). Determinants of Resident Tissue Macrophage Identity and Function. Immunity 52, 957–970. 10.1016/j.immuni.2020.05.014. [PubMed: 32553181]

30. Bohaud C, Johansen MD, Jorgensen C, Kremer L, Ipseiz N, and Djouad F (2021). The Role of Macrophages During Mammalian Tissue Remodeling and Regeneration Under Infectious and Non-Infectious Conditions. Front. Immunol 12, 707856. 10.3389/fimmu.2021.707856. [PubMed: 34335621]

31. Paolicelli RC, Bolasco G, Pagani F, Maggi L, Scianni M, Panzanelli P, Giustetto M, Ferreira TA, Guiducci E, Dumas L, et al. (2011). Synaptic pruning by microglia is necessary for normal brain development. Science 333, 1456–1458. 10.1126/science.1202529. [PubMed: 21778362]

32. Korn C, and Augustin HG (2015). Mechanisms of Vessel Pruning and Regression. Dev. Cell 34, 5–17. 10.1016/j.devcel.2015.06.004. [PubMed: 26151903]

33. Petrie TA, Strand NS, Yang CT, Rabinowitz JS, and Moon RT (2014). Macrophages modulate adult zebrafish tail fin regeneration. Development 141, 2581–2591. 10.1242/dev.098459. [PubMed: 24961798]

34. Vérollet C, Charrière GM, Labrousse A, Cougoule C, Le Cabec V, and Maridonneau-Parini I (2011). Extracellular proteolysis in macrophage migration: losing grip for a breakthrough. Eur. J. Immunol 41, 2805–2813. 10.1002/eji.201141538. [PubMed: 21953638]

35. Gong Y, Hart E, Shchurin A, and Hoover-Plow J (2008). Inflammatory macrophage migration requires MMP-9 activation by plasminogen in mice. J. Clin. Invest 118, 3012–3024. 10.1172/JCI32750. [PubMed: 18677407]
36. Travnickova J, Nhim S, Abdellaoui N, Djouad F, Nguyen-Chi M, Parmeggiani A, Kissa K. Macrophage morphological plasticity and migration is Rac signalling and MMP9 dependant. Sci. Rep 2021, 11, 10123, doi:10.1038/s41598-021-88961-7 (2021). [PubMed: 33980872]
37. Ellett F, Pase L, Hayman JW, Andrianopoulos A, and Lieschke GJ (2011). mpeg1 promoter transgenes direct macrophage-lineage expression in zebrafish. Blood 117, e49–e56. 10.1182/blood-2010-10-314120. [PubMed: 21084707]
38. Davies LC, Jenkins SJ, Allen JE, and Taylor PR (2013). Tissue-resident macrophages. Nat. Immunol 14, 986–995. 10.1038/ni.2705. [PubMed: 24048120]
39. Rostam HM, Reynolds PM, Alexander MR, Gadegaard N, and Ghaemmaghami AM (2017). Image based Machine Learning for identification of macrophage subsets. Sci. Rep 7, 3521. 10.1038/s41598-017-03780-z. [PubMed: 28615717]
40. Vereyken EJF, Heijnen PDAM, Baron W, de Vries EHE, Dijkstra CD, and Teunissen CE (2011). Classically and alternatively activated bone marrow derived macrophages differ in cytoskeletal functions and migration towards specific CNS cell types. J. Neuroinflammation 8, 58. 10.1186/1742-2094-8-58. [PubMed: 21615896]
41. Roh-Johnson M, Shah AN, Stonick JA, Poudel KR, Kargl J, Yang GH, di Martino J, Hernandez RE, Gast CE, Zarour LR, et al. (2017). Macrophage-Dependent Cytoplasmic Transfer during Melanoma Invasion In Vivo. Dev. Cell 43, 549–562.e6. 10.1016/j.devcel.2017.11.003. [PubMed: 29207258]
42. Kuil LE, Oosterhof N, Ferrero G, Mikulášová T, Hason M, Dekker J, Rovira M, van der Linde HC, van Strien PM, de Pater E, et al. (2020). Zebrafish macrophage developmental arrest underlies depletion of micro-glia and reveals Csf1r-independent metaphocytes. Elife 9, e53403. 10.7554/eLife.53403. [PubMed: 32367800]
43. Curado S, Stainier DYR, and Anderson RM (2008). Nitroreductase-mediated cell/tissue ablation in zebrafish: a spatially and temporally controlled ablation method with applications in developmental and regeneration studies. Nat. Protoc 3, 948–954. 10.1038/nprot.2008.58. [PubMed: 18536643]
44. Pisharath H, and Parsons MJ (2009). Nitroreductase-mediated cell ablation in transgenic zebrafish embryos. Methods Mol. Biol 546, 133–143. 10.1007/978-1-60327-977-2_9. [PubMed: 19378102]
45. Parichy DM, Elizondo MR, Mills MG, Gordon TN, and Engeszer RE (2009). Normal table of postembryonic zebrafish development: staging by externally visible anatomy of the living fish. Dev. Dynam 238, 2975–3015. 10.1002/dvdy.22113.
46. Ando K, Shibata E, Hans S, Brand M, and Kawakami A (2017). Osteoblast Production by Reserved Progenitor Cells in Zebrafish Bone Regeneration and Maintenance. Dev. Cell 43, 643–650.e3. 10.1016/j.devcel.2017.10.015. [PubMed: 29103952]
47. Hirata M, Nakamura K.i., Kanemaru T, Shibata Y, and Kondo S (2003). Pigment cell organization in the hypodermis of zebrafish. Dev. Dynam 227, 497–503. 10.1002/dvdy.10334.
48. Lagente V, Le Quement C, and Boichot E (2009). Macrophage metal-loelastase (MMP-12) as a target for inflammatory respiratory diseases. Expert Opin. Ther. Targets 13, 287–295. 10.1517/14728220902751632. [PubMed: 19236151]
49. Nighot M, Ganapathy AS, Saha K, Suchanec E, Castillo EF, Gregory A, Shapiro S, Ma T, and Nighot P (2021). Matrix Metalloproteinase MMP-12 Promotes Macrophage Transmigration Across Intestinal Epithelial Tight Junctions and Increases Severity of Experimental Colitis. J. Crohns Colitis 15, 1751–1765. 10.1093/ecco-jcc/jjab064. [PubMed: 33836047]
50. Pedersen ME, Vuong TT, Rønning SB, and Kolset SO (2015). Matrix metalloproteinases in fish biology and matrix turnover. Matrix Biol. 44–46, 86–93. 10.1016/j.matbio.2015.01.009.
51. Pagán AJ, Yang CT, Cameron J, Swaim LE, Ellett F, Lieschke GJ, and Ramakrishnan L (2015). Myeloid Growth Factors Promote Resistance to Mycobacterial Infection by Curtailing Granuloma Necrosis through Macrophage Replenishment. Cell Host Microbe 18, 15–26. 10.1016/j.chom.2015.06.008. [PubMed: 26159717]

52. Lee RTH, Asharani PV, and Carney TJ (2014). Basal keratinocytes contribute to all strata of the adult zebrafish epidermis. PLoS One 9, e84858. 10.1371/journal.pone.0084858. [PubMed: 24400120]

53. Gibson DG, Young L, Chuang RY, Venter JC, Hutchison CA 3rd, and Smith HO (2009). Enzymatic assembly of DNA molecules up to several hundred kilobases. Nat. Methods 6, 343–345. 10.1038/nmeth.1318. [PubMed: 19363495]

Highlights

- Metaphocytes are responsible for airineme-mediated signaling in zebrafish
- Metaphocytes relay airineme vesicles in hypodermis during metamorphosis
- Metaphocyte deficiency disrupts airineme-mediated signaling and pigment pattern
- Metaphocyte migration and their role in airineme signaling are MMP9 dependent

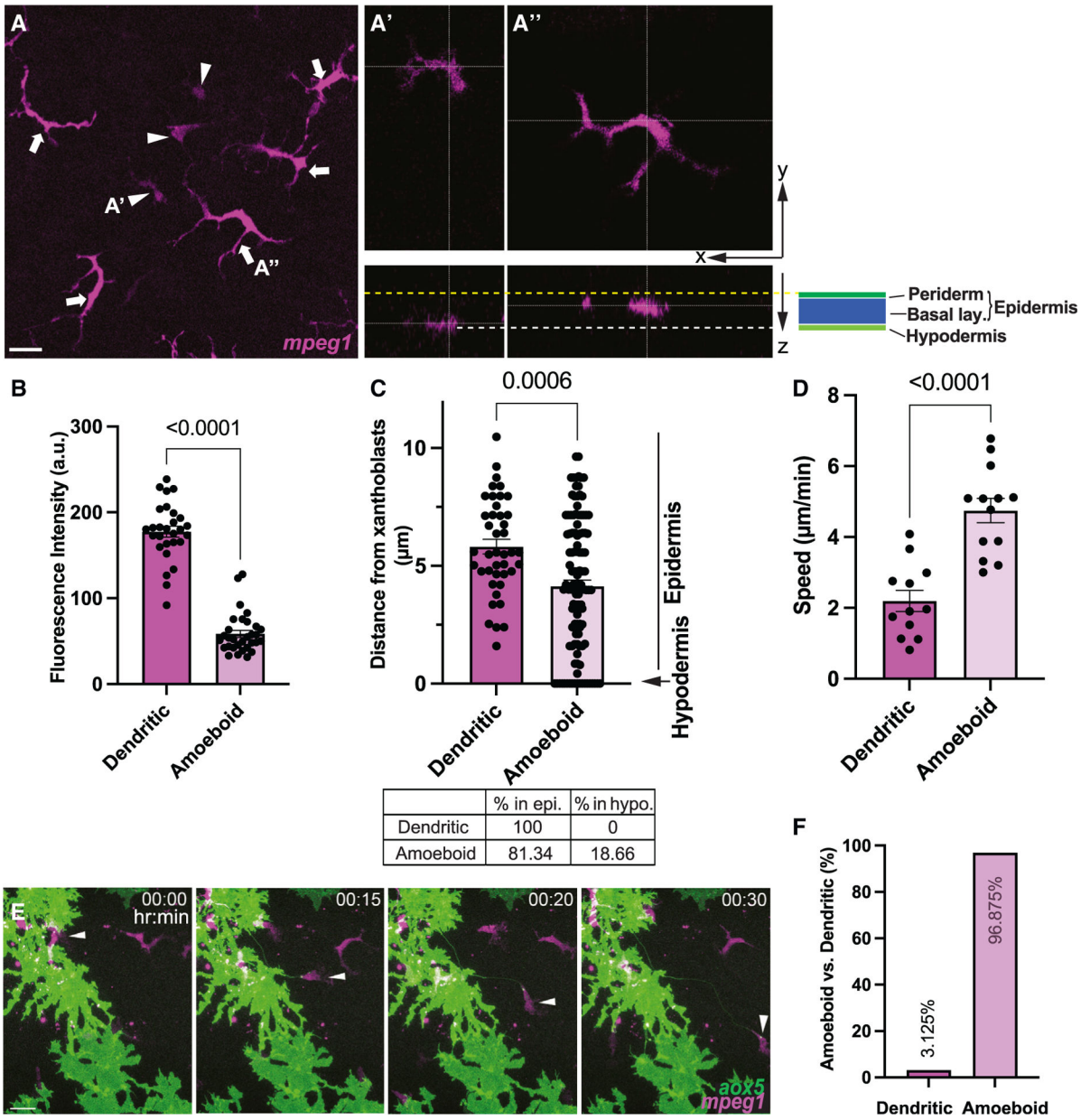

Figure 1. Two distinct macrophage subpopulations in zebrafish skin

(A) *mpeg1*+ ameboid (arrowheads) and dendritic (arrows) macrophages shown in maximum projection image. (A′) Ameboid macrophages at hypodermis. (A″) Dendritic macrophages at epidermis. Yellow dotted line denotes apical margin of epidermis. White dotted line denotes hypodermal layer. Epidermis comprises both periderm and basal layer (see Figure S1).

(B) Significantly lower *mpeg1* expression in ameboid population compared to the dendritic population; n = 28 dendritic, n = 31 ameboid cells.

(C) Ameboid macrophages are localized more basally than dendritic and reach hypodermis (arrow); n = 63 dendritic, n = 122 ameboid cells.

(D) Migration speed of dendritic and ameboid macrophages; n = 12 dendritic, n = 13 ameboid cells.
(E) Airinemes are pulled by ameboid macrophages (arrowheads). Still images from time-lapse movie.
(F) Percentages of airineme-pulling macrophage subpopulations. Statistical significances were assessed by Student t test. Scale bars, 20 mm. Bars display mean, and error bars display SEM.

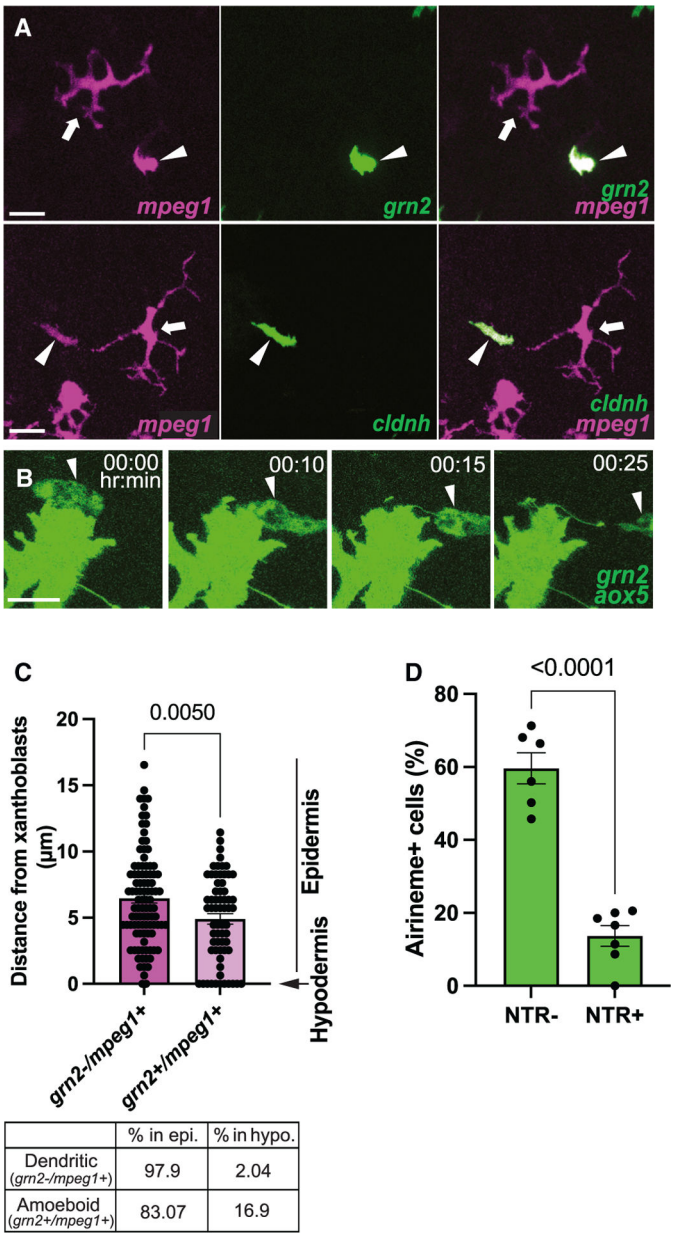

	% in epi.	% in hypo.
Dendritic (*grn2-/mpeg1+*)	97.9	2.04
Amoeboid (*grn2+/mpeg1+*)	83.07	16.9

Figure 2. Airineme pulling ameboid macrophages overlap with ectoderm-derived metaphocytes

(A) Coexpression of metaphocyte markers, *grn2* and *cldnh*, in ameboid macrophage subpopulation (*mpeg1*+, arrowheads). Note that dendritic (*mpeg1*+, arrows) macrophages do not express metaphocyte markers.

(B) Still images from a time-lapse movie showing airinemes being pulled by *grn2*+ metaphocytes.

(C) Similar to the ameboid macrophage population, metaphocytes are more frequently located in the hypodermis.

(D) Airineme extension was quantified by counting the number of cells that extended airinemes at least once out of all imaged cells. Xanthoblasts of metaphocyte depleted fish (NTR+) were less likely than controls (NTR–) to extend airinemes; n = 6 (controls), n

= 7 (depleted) time-lapse positions, three trunks each. The few airinemes extended in the depleted were associated with residual metaphocytes (Video S4). Statistical significances were assessed by Student t test. Scale bars, 20 μm (A), 10 μm (B). Bars display mean, and error bars display SEM.

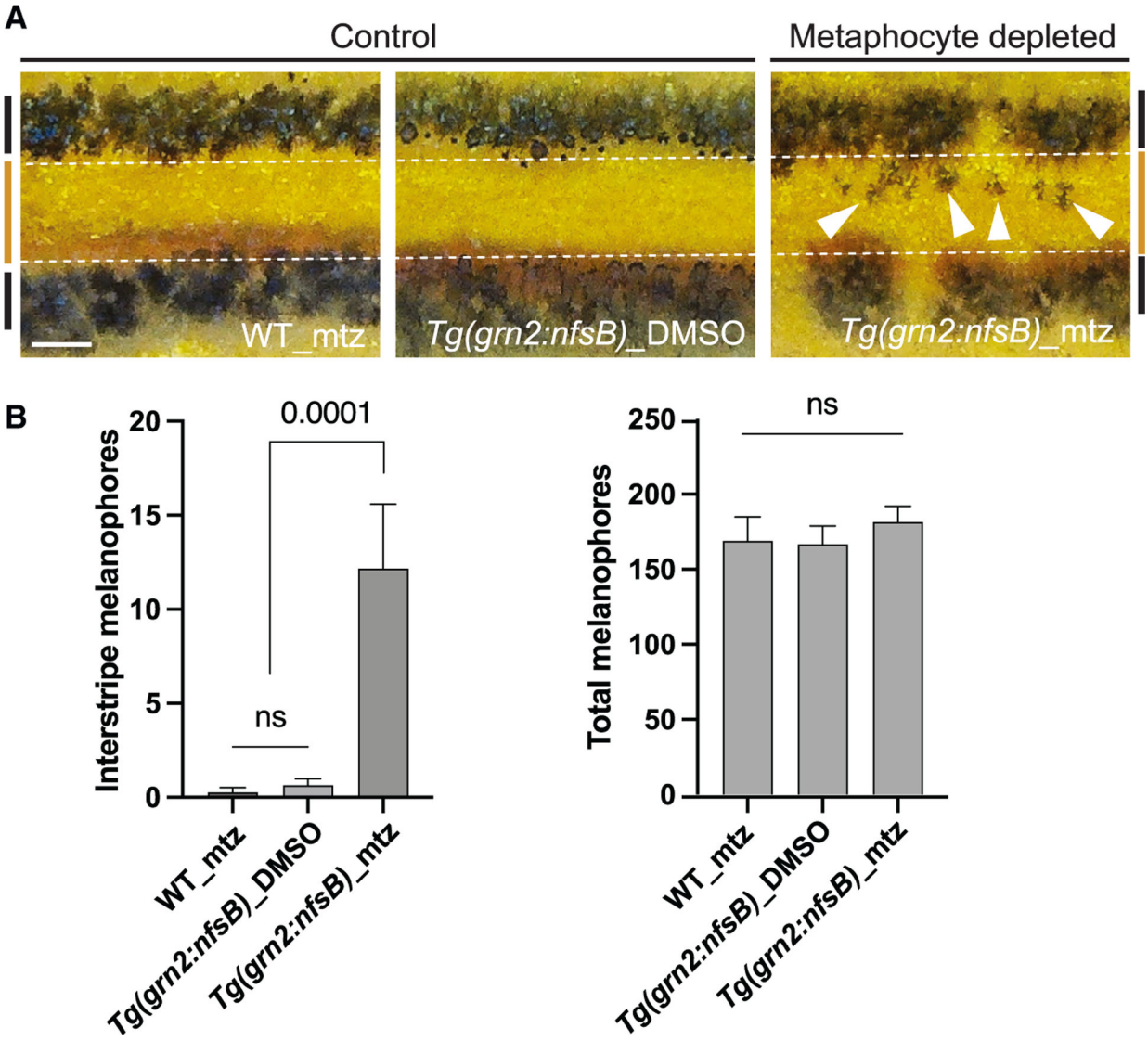

Figure 3. Metaphocyte-mediated airineme extension is responsible for melanophore pattern formation

(A) In two controls, melanophores reside in the stripe region (denoted by black bars at far left and right, and white dotted lines) and the border of the interstripe (orange bar). Metaphocyte depletion results in melanophores retention in the interstripe (arrowheads). (B) Numbers of melanophores in the interstripe. Metaphocyte-depleted fish (*Tg(grn2:nfsB)*_mtz) had significantly more melanophores in the interstripe than the controls (WT_mtz and *Tg(grn2: nfsB)*_DMSO) and displayed a disorganized pigment pattern, although total melanophore numbers did not differ; data are means ± SEM. At stage 12, standardized standard length (SSL); n = 4, WT_mtz, n = 15, *Tg(grn2:nfsB)*_DMSO, n = 11, *Tg(gnr2:nfsB)_mtz* trunks. Statistical significances were assessed by Student t test. Scale bar, 200μm (A). mtz, metronidazole.

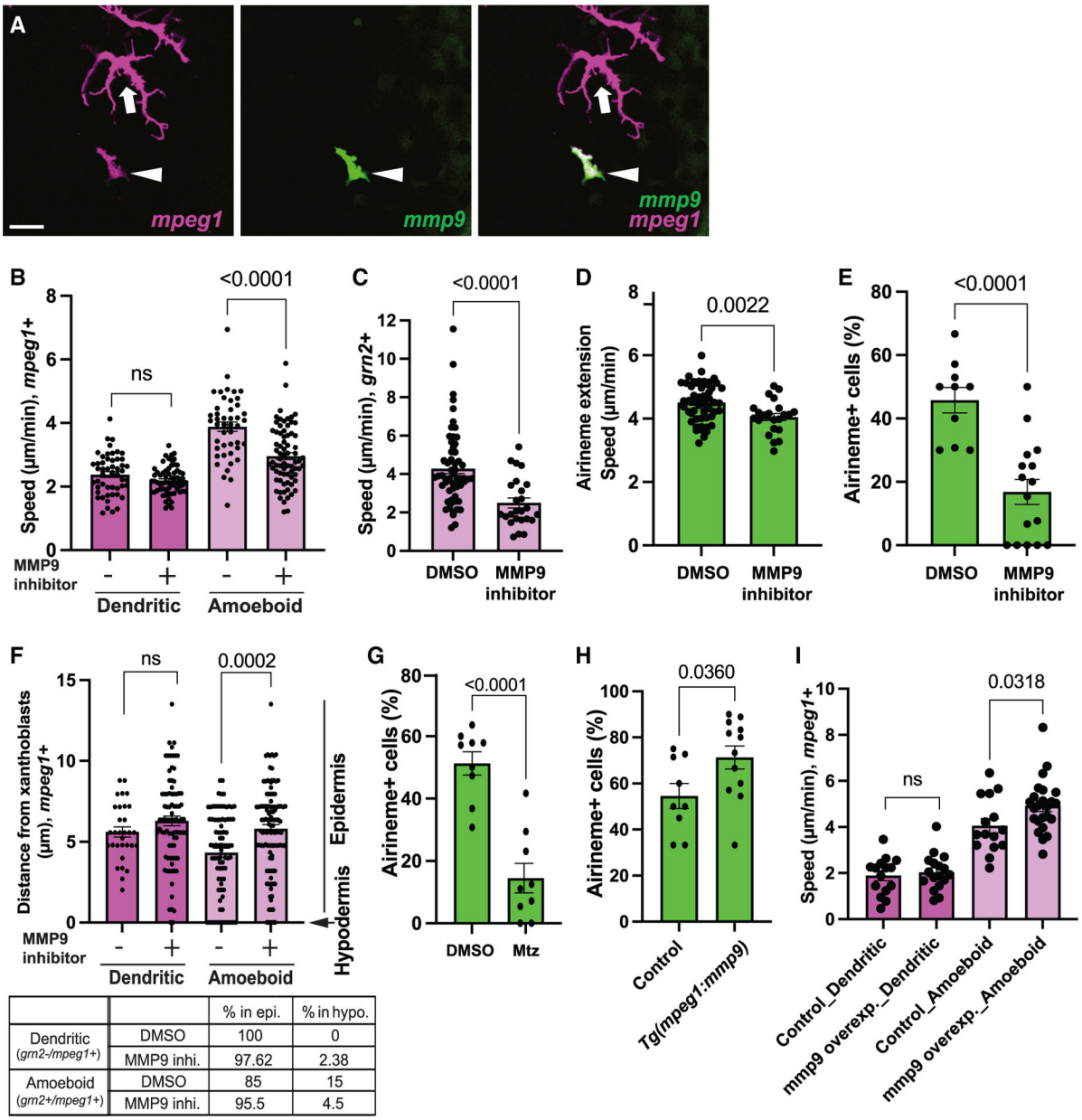

		% in epi.	% in hypo.
Dendritic (*grn2-/mpeg1+*)	DMSO	100	0
	MMP9 inhi.	97.62	2.38
Amoeboid (*grn2+/mpeg1+*)	DMSO	85	15
	MMP9 inhi.	95.5	4.5

Figure 4. MMP9 manipulations affect metaphocyte migration speed and airineme extension frequency

(A) Differential expression of MMP9 in ameboid (arrowhead) and dendritic macrophage subpopulation (arrow).

(B) Treatment with an MMP9 inhibitor significantly reduced the migration speed of the ameboid macrophage subpopulation, while dendritic macrophages were unaffected (n = 51, 64, 45, and 68 cells), four trunks each. *The n numbers represent the experimental groups from left to right order for all the following figure legends.

(C) Consistently, the migration speed of *grn2+* metaphocytes was significantly decreased in MMP9 inhibitor-treated fish (n = 28 and 31 cells; 4 trunks each).

(D) Airineme extension speed reduction in the presence of MMP9 inhibitor (n = 53 and 23; 3 trunks each).

(E) Xanthoblasts in MMP9 inhibitor treated fish had fewer airinemes than controls (n = 10 and 16 time-lapse positions; 4 and 5 trunks).
(F) Localization of ameboid macrophages were shifted more apically upon MMP9 inhibitor treatment but no effects on dendritic macrophage subpopulation (n = 31, 45, 80, and 75 cells; 3, 3, 4, and 5 trunks).
(G) Xanthoblasts in mmp9+ cell-depleted fish had fewer airinemes than controls (n = 9 and 9 time-lapse positions; 3 trunk each).
(H) Xanthoblasts in mmp9 overexpressed fish extend more airinemes than controls (n = 9 and 12 time-lapse positions; 4 trunk each).
(I) The migration speed of the ameboid macrophage subpopulation was increased, while dendritic macrophages remained unaffected (n = 15, 17, 15, and 24 cells; 3 trunk each). Scale bar, 20 μm (A). Statistical significances were assessed by Student t test. Bars display mean, and error bars display SEM.

KEY RESOURCES TABLE

REAGENT or RESOURCE	SOURCE	IDENTIFIER
Chemicals, Peptides, and Recombinant Proteins		
DMSO	Sigma-Aldrich	D8418
metronidazole	Sigma-Aldrich	M3761
MMP9 inhibitor II	Calbiochem	44–429-310MG
Critical Commercial Assays		
LR Clonase II	Invitrogen	12538120
Gibson Assembly®Master Mix	NEB	E2611L
SuperScript™ III Reverse Transcriptase	Invitrogen	18080093
Experimental Models: Organisms/Strains		
Zebrafish: ABb wild-type	Parichy lab	N/A
Zebraf ish: *Tg(cldn3c:GFP)hkz021tTg*	Wen lab	ZFIN: ZDB-ALT-191122–2
Zebrafish: *Tg(mpeg1:loxp-DsRedxloxp-EGFP)hkz015tTg*	Wen lab	ZFIN:ZDB-ALT-161018–7
Zebrafish: *TgBAC(grn2:EGFP-NTR)hkz034Tg*	Wen lab	ZFIN:ZDB-ALT-210708–2
Zebrafish: *Tg(tyrp 1b:PALMmCherry)wprt11Tg*	Parichy lab	ZDB-ALT-141218–2
Zebrafish:Tg(mpeg1.1:LOX2272-LOXP-dTomato-LOX2272-Cerulean-LOXP-EYFP)w201Tg	Ramakrishnan Lab	ZDB-ALT-150512–3
Zebrafish: *TgBAC(mmp9:EGFP)tyt206Tg*	Kawakami Lab	ZDB-ALT-180501–1
Zebrafish: *TgBAC(mmp9:EGFP-NTR)tyt207Tg*	Kawakami Lab	ZDB-ALT-180501–2
Zebrafish: *Tg(mpeg1:mmp9-v2a-nVenus)irrt15Tg*	This paper	N/A
Zebrafish: *Tg(krt4:PALMegfp)irrt1Tg*	This paper	N/A
Zebrafish: *Tg(krtt1c19e:LY-Tomato)sq16Tg*	Carney lab	ZDB-ALT-140424–2
Oligonucleotides		
*aox5*_forward, 5′-CAGAGTGACGTCTGGTCTTACG-3′	This paper	N/A
*aox5*_reverse, 5′-GGACATCTGATAGCCACACTTG-3′	This paper	N/A
*pmela*_forward, 5′-CICGGAGIICIGIIIIICGIII-3′	This paper	N/A
*pmela*_reverse, 5′-AAGGTACTGCGCTTATTCCTGA-3′	This paper	N/A
*actin*_forward, 5′-CTTGCTCCTTCCACCATGAA-3′	This paper	N/A
*actin*_reverse, 5′-CTGCTTGCTGATCCACATCT-3′	This paper	N/A
*mmp9*_forward, 5′-CATTAAAGATGCCCTGATGTATCCC-3′	This paper	N/A
*mmp9*_reverse, 5′-AGTGGTGGTCCGTGGTTGAG-3′	This paper	N/A
Recombinant DNA		
cldnh:mCherry	This paper	N/A